Structural Engineering and Mechanics, Vol. 35, No. 1 (2010) 99-117
DOI: http://dx.doi.org/10.12989/sem.2010.35.1.099

Experiments on reinforced concrete beam-column joints under cyclic loads and evaluating their response by nonlinear static pushover analysis

Akanshu Sharma[1]*, G.R. Reddy[1], Rolf Eligehausen[2], K.K. Vaze[1], A.K. Ghosh[1] and H.S. Kushwaha[3]

[1]Reactor Safety Division, Bhabha Atomic Research Centre, Trombay, Mumbai-400085, India
[2]Institut für Werkstoffe im Bauwesen, Universität Stuttgart, Pfaffenwaldring 4, 70569 Stuttgart, Germany
[3]Health Safety & Environment Group, Bhabha Atomic Research Centre, Trombay, Mumbai-400085, India

(Received May 23, 2008, Accepted January 22, 2010)

Abstract. Beam-column joints are the key structural elements, which dictate the behavior of structures subjected to earthquake loading. Though large experimental work has been conducted in the past, still various issues regarding the post-yield behavior, ductility and failure modes of the joints make it a highly important research topic. This paper presents experimental results obtained for eight beam-column joints of different sizes and configuration under cyclic loads along with the analytical evaluation of their response using a simple and effective analytical procedure based on nonlinear static pushover analysis. It is shown that even the simplified analysis can predict, to a good extent, the behavior of the joints by giving the important information on both strength and ductility of the joints and can even be used for prediction of failure modes. The results for four interior and four exterior joints are presented. One confined and one unconfined joint for each configuration were tested and analyzed. The experimental and analytical results are presented in the form of load-deflection. Analytical plots are compared with envelope of experimentally obtained hysteretic loops for the joints. The behavior of various joints under cyclic loads is carefully examined and presented. It is also shown that the procedure described can be effectively utilized to analytically gather the information on behavior of joints.

Keywords: beam-column joints; cyclic loading; nonlinear static pushover analysis; strength; ductility.

1. Introduction

It has been recognized world over that, in reinforced concrete structures subjected to earthquake type excitation, beam-column junction is an important structural element (Pauley and Priestley 1992). The joint consists mainly of three components, beam (along with the slab, if any), column, and the joint core (generally considered as a part of column). The characteristics and behavior of the joint therefore depends on the behavior of these three components. The seismic moments in the columns immediately above and below the joint and similar beam moment reversals across the joint induce huge horizontal and vertical forces in the joint core. Various standard codes (ACI318 2008, EuroCode8 2003, NZS 3101 1995, IS 1893 2002) give certain guidelines to provide additional

*Corresponding author, Scientific Officer, E-mail: akanshusharma@yahoo.co.in, akanshu@barc.gov.in

reinforcement in the joint core, which can prevent the joint shear failure. However, many a times the failure of a joint commences from the flexural, or less commonly, shear failure of beams or columns across the joint and gradually the cracks developed in beams and columns propagate into the joint. In addition to reinforcement in joint core, the standards specify closely spaced stirrups and longer development lengths for beams and columns in order to provide a ductile failure mode. Although the minimum strength and ductility requirements are deemed to be satisfied if one follows the guidelines, a simple analytical method that can predict the strength and ductility of the joints (or structures), reasonably accurately, can be an excellent design verification tool. The simple analytical model based on well known Pushover Analysis presented in this chapter is one such tool that can be easily followed for verification of performance of the joints or structure. It is shown that even the cyclic behavior of the joints can be predicted by such analysis and also the failure modes be predicted by the analysis.

In this research work, the behavior of different sized joints with different types of reinforcement detailing was investigated. The experimental load-displacement hysteretic loops for eight beam column joints are presented. Out of eight, four joints had confined seismic reinforcement detailing (IS 1893 2002) and four joints had unconfined non-seismic detailing (IS 456 2000). Again four joints were interior (cross-shaped) and four joints were exterior (tee-shaped) in configuration. Sizes of members in joints varied from 150 mm × 200 mm to 400 mm × 500 mm. The most interesting observation in this work was that the effect of detailing on the performance of joints is more pronounced for smaller joints than on larger joints. However, in order to have a wider database and acceptance, further tests on similar lines need to be planned for better insight on the subject.

More and more people now advocate following nonlinear analysis procedures and evaluating the overall performance of the structure instead of just concentrating on the strength of the structure. However, the complete nonlinear dynamic time-history analysis is still found too complex to be applied to real life structures. Consequently, nonlinear static analysis procedure, which gives a good trade off between accuracy of nonlinear analysis and simplicity of static analysis, is gaining popularity. In this work, therefore, an attempt was made to analyze all the joints using nonlinear static pushover analysis technique to obtain the monotonic load-displacement plot. This analytical plot was compared with the envelope of experimental hysteretic loops. It was found that the analytical plots obtained by the procedure presented in the paper are capable of providing a good estimate of available strength and ductility in the joints. Thus, the procedure described here can be effectively used to predict the performance of the joint under cyclic loads.

2. Research significance

Although both the topics namely “behavior of reinforced concrete beam-column joints under cyclic loads” and “nonlinear static pushover analysis” have interested researchers for quite some time now, any attempt to evaluate the former using the latter is not known to the authors. Moreover, most of the tests performed in the past by researchers to study the effect of detailing on behavior of joints is limited to small-scale specimens. This work is therefore an attempt to address the following two issues

(i) Evaluating experimentally the behavior of laboratory scale and real life scale RC beam-column joints under cyclic loads
(ii) Developing a simple and effective analytical procedure for evaluation of the behavior of RC beam-column joints and validate the procedure against experimental results

3. Literature review

Significant research has gone into understanding the behavior of beam-column joints under earthquake type loads. Hanson and Connor (1967) studied the behavior of small-sized exterior beam-column joints. They demonstrated that a joint without transverse reinforcement could not sustain much load after the third moderate cycle of reversed loading. Renton (1972) conducted tests on specimens with different joint tie content and form of anchorage of the beam reinforcement. As per conclusions given by Park and Pauley (1975) for these tests, "not one specimen attained the theoretical flexural capacity; the degradation of strength was also notable. It was concluded that additional shear reinforcement would serve no useful purpose and that only a radical change in the geometry of the joint could hold some promise for improvement." Park and Thompson (1974) conducted tests on ductile detailed joints with 9 inches × 18 inches beam and 12 inches by 16 inches columns and they observed unsatisfactory joint behavior. Lee *et al.* (1977) conducted experiments on beam-column joints, member size 8 inches × 10 inches, with ductile and non-ductile detailing. The ductility for both ductile and non-ductile detailed joints was found to be around 5, however, the specimen with ductile detailing formed better hysteretic loops and dissipated more energy. Leon (1990) reported experimental results of cyclic tests on three reinforced concrete beam-column joints with beam sizes of 8 inches × 12 inches and column sizes varying from 10 inches × 10 inches to 14 inches × 10 inches, with closely spaced stirrups. The ductility ratios were found in the range of 3 to 3.5. Raffaelle and Wight (1995) tested four eccentric beam-column connections with beam section dimensions of around 10 inches × 15 inches, and shear reinforcements at a spacing of around 80 mm c/c. The ductility was of the order of 2.5. More recently, Satish Kumar and Vijaya Raju (2002) conducted experiments on beam-column joints, member sizes 150 mm × 200 mm with ductile detailing as prescribed by Indian Standard (IS 2002), under monotonic and cyclic loads. The ductility values varied from around 2.5 to 6. Megget (2003) studied the seismic performance of eleven half-scale and three full-sized reinforced concrete beam-column knee joints under inelastic cyclic loading. Twelve joints were designed to the New Zealand Concrete Standard (NZS 1995), while the remaining two were designed to the 1964 New Zealand Code, which contained few seismic provisions. All the new designs approached or exceeded their nominal beam strengths in both directions and only degraded in strength at displacement ductility factors greater than 2, while the older designs failed prematurely in joint shear at about 70% of the beam nominal strengths.

Thus, it can be seen that many people have done large research work on the behavior of RC beam column joints but their conclusions varied to a large extent especially on the front of ductility. This may be due to the fact that different people conducted experiments on joints of different sizes and configurations.

4. Beam-column joint mechanics

When RC moment frames are subjected to lateral seismic loading, high shear forces are generated in the joint core. Figs. 1 and 2 show the mechanics of exterior and interior joints respectively when subjected to seismic forces (Paulay and Priestley 1992). Here the length of the beam L_b is half of the bay width and L_c is the storey height. The other dimensions are explained in the figure.

A system of diagonal compression strut and tension tie is developed in the concrete core to

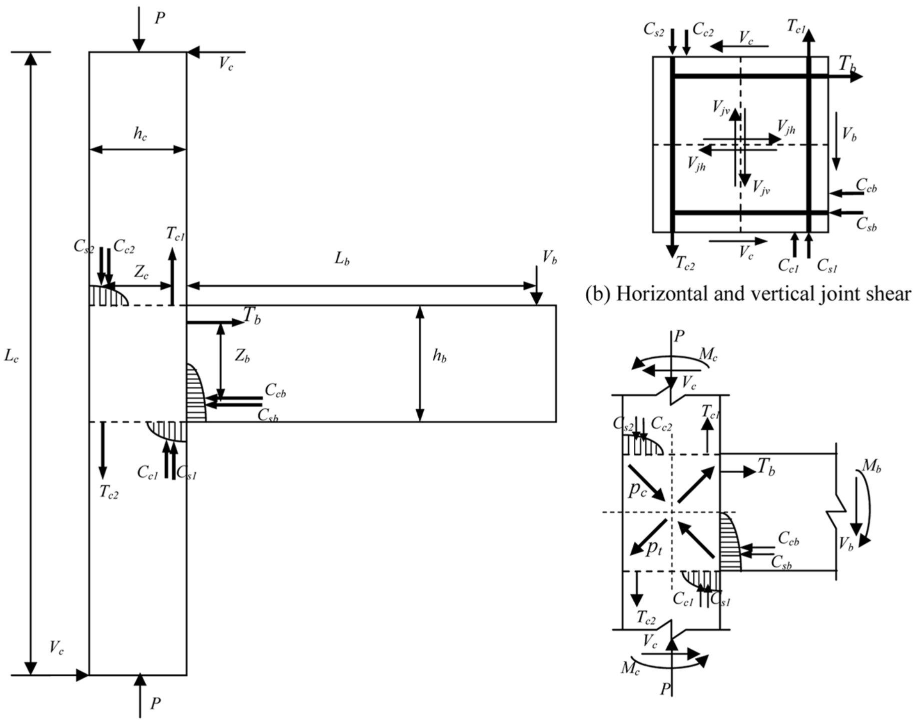

(b) Horizontal and vertical joint shear

(a) External actions and forces in beams and columns (c) Principal stresses in joint

Fig. 1 Mechanics of exterior joint under seismic actions

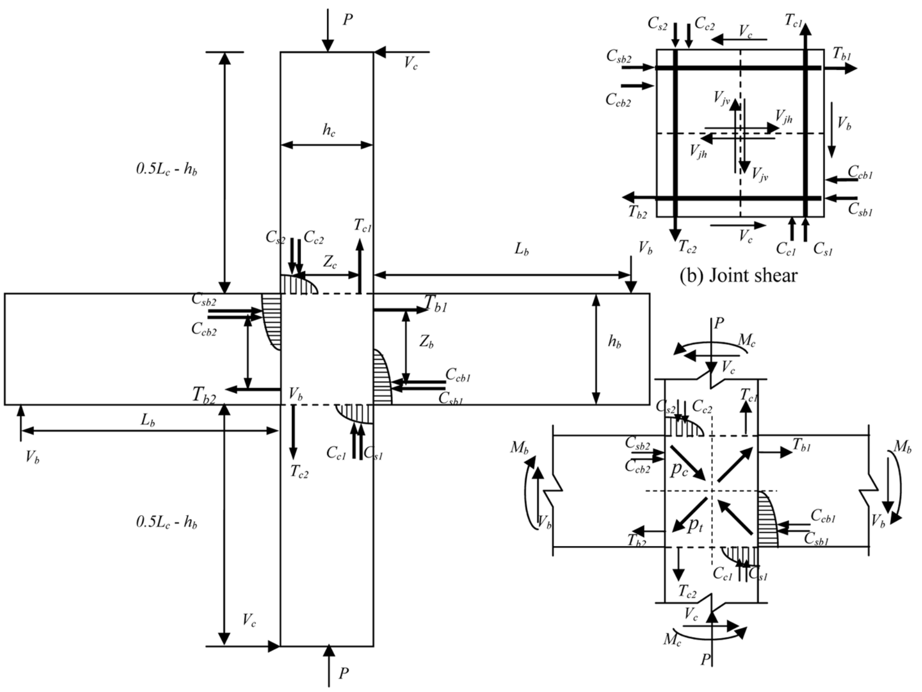

(b) Joint shear

(a) External actions and forces in beams and columns (c) Principal stresses in joint

Fig. 2 Mechanics of interior joint under seismic actions transmit the joint shear forces. Some of the internal forces, particularly those generated in the concrete will combine to develop a diagonal strut (Paulay and Priestley 1992). Other forces transmitted to the joint core from beam and column bars by means of bond, necessitate a truss mechanism. The strength of this diagonal strut controls the joint strength before cracking. The transverse reinforcement in the joint helps confine the concrete diagonal strut in the joint core thereby contributing to increased joint strength. If the joint shear forces are large, diagonal cracking in the joint core occurs followed by the crushing of concrete in joint core. The joint reinforcement alone is not sufficient to avoid undesirable pinching in hysteretic loops at this stage (Murty *et al.* 2003).

Standards such as ACI 318 (2008) and NZS 3101 (1995) recommend to keep the stresses in the joint below permissible limits. ACI 318 specifies this limit based on the tensile strength of concrete by specifying the value of maximum permissible horizontal joint shear stress as $k\sqrt{f_c'}$, where, f_c' is the cylinder compressive strength of concrete and k is a parameter that depends on the confinement provided by the members framing into the joint. It is sometimes argued (Hakuto *et al.* 2000) that the tension cracking criteria may be too conservative and the joint core may be capable of transferring significantly higher shear forces after diagonal tension cracking also, by means of diagonal compression strut mechanism. NZS 3101 (1995) recognizes this approach and specifies that to avoid diagonal compression failure in the joints, the horizontal shear stress shall not exceed a value of 0.2 f_c'.

It is now recognized that principal stresses, which consider the contribution of axial forces also, provide better criteria for the damage in the joint (Priestley 1997, Pampanin *et al.* 2003). The values are prescribed as $k\sqrt{f_c'}$, where, f_c' is the cylinder compressive strength of concrete and k is a parameter that depends on the type of joint, type of reinforcement and end anchorage details. Priestley (1997) suggested the critical principal tensile stress values for exterior and corner beam-column joints with deformed bars with bent-in and bent-out type end anchorages and Pampanin *et al.* (2003) have suggested the same for exterior beam-column joints with plain round bars and end hooks.

5. Experimental programme

The various parameters to describe a joint are tabulated in Table 1 below. Joints 1 and 2 were tested at IIT Bombay (Mukherjee 2006), Joints 3 and 4 were tested at IIT Kanpur (Jain and Murty 1999) and joints 5 through 8 were tested at SERC, Chennai (Thandavamoorty *et al.* 2006). Joints 1, 2, 3 and 4 were specially designed for laboratory testing while joints 5, 6, 7 and 8 were replicated from the actual joints present in real life office buildings. Cold worked deformed bars were used for all the joints except where the reinforcement size is 6 mm or lower for which Mild steel was used. All dimensions are in mm. Fig. 3 shows the meaning of symbols diagrammatically for exterior joints and Fig. 4 does the same for interior joints. Fig. 3 shows the actual experimental setup used for testing of the specimens. Some of the joints were having a strong beam – weak column configuration, while others were having strong column – weak beam configuration. Although it is true that in real life the beams are invariably flanged beams and that this effect shall be considered while deciding on the configuration of the joints, yet in this case it was not considered since, there were no slabs modeled in the tests. Also, since seismic loading is reversing, therefore the effect of slab on the strength of the beam in one direction (causing tension in the slab) cannot be considered.

Table 1 Details of specimens tested

Joint No.	C/U*	E/I#	L_b	$0.5L_c–h_b$	Beam size		Column Size		f_{ck} (MPa)	% Long Reinft		Trans Reinft (Dia-c/c spacing)	
					b_b	h_b	b_c	h_C		Beam	Column	Beam	Column
1	U	I	600	800	150	200	150	200	34.33	1.51	2.68	6-150	6-150
2	C	I	600	800	150	200	150	200	34.33	1.51	2.68	6-75	6-75
3	U	E	1180	700	200	400	200	250	47.2	1.57	1.61	8-270	8-250
4	C	E	1180	700	200	400	200	250	38.2	1.57	1.61	8-90	8-75
5	U	I	1360	1700	400	400	400	400	50.95	5.09	1.57	16-125	6-280
6	C	I	1360	1700	400	400	400	400	40.71	5.09	1.57	16-125	6-150
7	U	E	1760	1555	400	500	400	470	41.61	5.09	1.52	8-175	6-190
8	C	E	1760	1555	400	500	400	470	35.86	5.09	1.52	12-125	6-90

*Confined/Unconfined
#Exterior/Interior

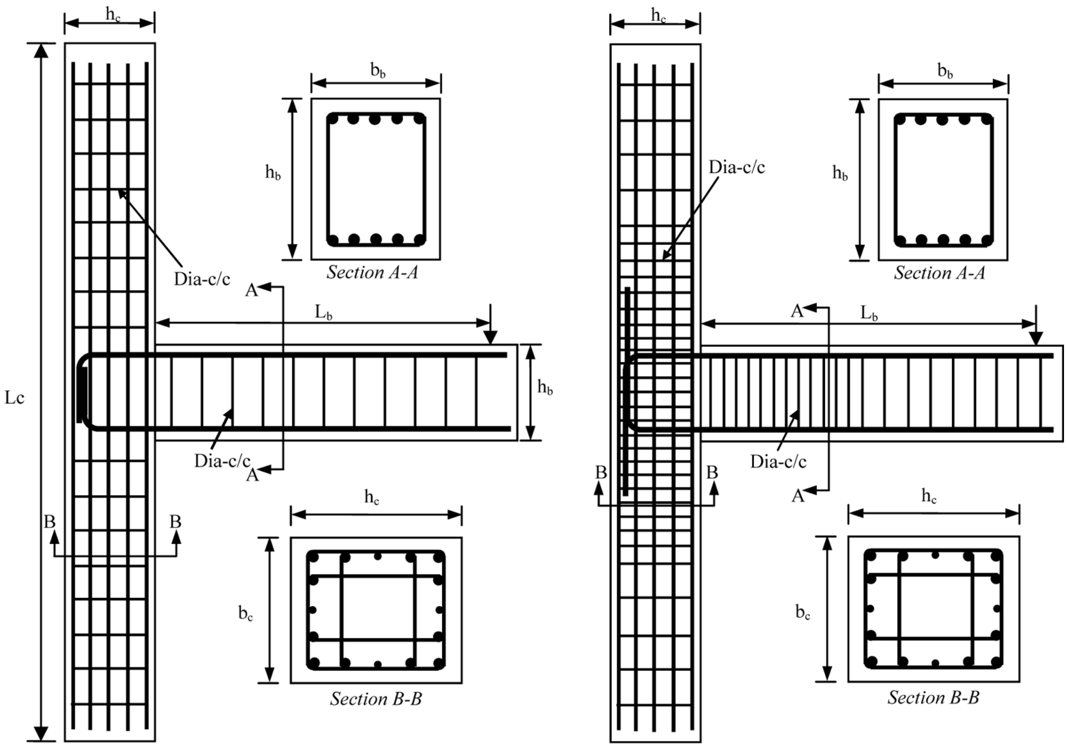

(a) Unconfined Joint (b) Confined Joint

Fig. 3 Details of exterior joints

Therefore, in this case, the configuration, i.e., whether the joint belongs to a strong beam-weak column or strong column-weak beam configuration is judged on the basis of hierarchy of strength in the sub-assemblage.

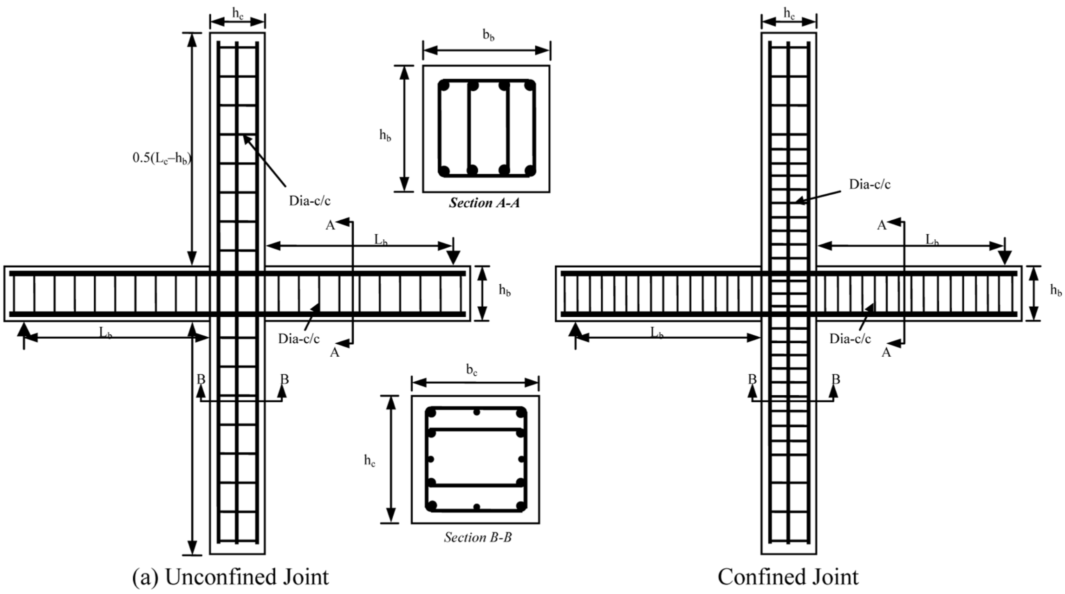

Fig. 4 Details of interior joints

6. Analytical procedure

The analysis of the joints was performed using nonlinear static pushover analysis procedure to obtain the monotonic load-displacement plots. The procedure is based on classical approach where, moment-rotation and shear force-deformation characteristics are first derived for the section under consideration. These characteristics are then assigned to the potential hinge formation locations in the structure (e.g., very close to the fixed end of a cantilever beam).

To model the nonlinearity in the joint, the failure criteria can be based either on the horizontal joint shear stress as recommended by codes such as ACI 318 (2008) or the principal tensile stress approach as proposed by Priestley (1997). In this case the joint characteristics were based on the criteria suggested by FEMA 356 (2000). The load on the beam corresponding to the permissible values of joint shear stress was calculated following the principles of statics and the equivalent moment-rotation was assigned to the members as explained later.

The first set of analysis of the structure under a set of loads is performed within linear range, i.e., all the members are within elastic range, and the forces/moments at critical locations are obtained. The load is then gradually increased, till the forces/moments at certain locations (where hinge properties are already assigned) become equal to the yield forces/moments. At this point the displacement of the structure is recorded. As the forces/moments at the potential hinge locations exceed the yield value, the stiffness matrix of the structure is modified to take into account the redistribution of forces within the members of the structure. The structure is again analyzed to get the new set of forces/moments and the load is again increased till yield values of forces/moments are reached at certain other locations, and the displacements are again recorded. The procedure is repeated till, either the required level of displacement is obtained, or the structure reaches forms a collapse mechanism.

The same procedure, as described above, was followed to track the load *v/s* deformation plot for

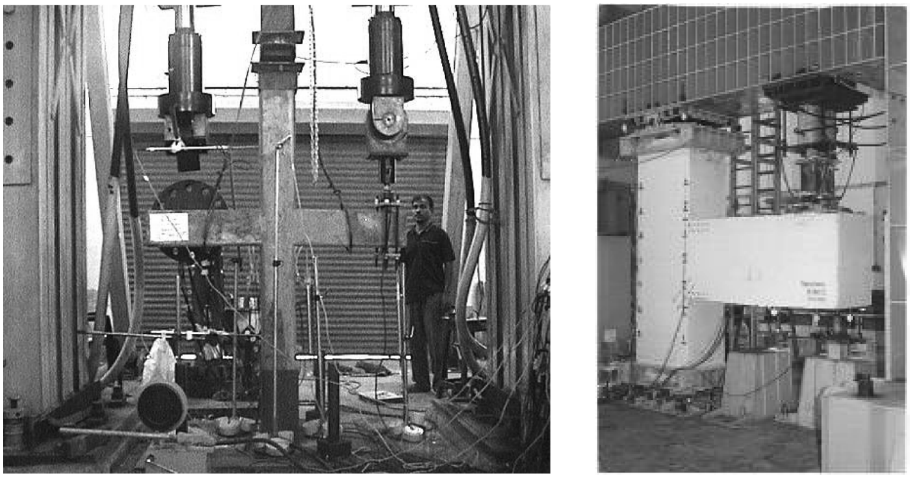

Fig. 5 Experimental setup used for testing of joint specimen

the beam-column joint sub-assemblage. It is to be noted that in this work, both the shear force-deformation characteristics were generated and assigned to the members. However, for flexural members with high shear span to depth ratio (more than 6), the shear force-deformation hinges are redundant as their contribution for such members is negligible as compared to the contribution of the flexural deformations. Nevertheless, in such cases also, it must be ensured that the shear capacity of the member is significantly higher than the flexural capacity, lest the shear failure mode dominates.

The procedure followed to obtain the member hinge properties is described under.

6.1 Moment-rotation characteristics

The stress-strain characteristics of a concrete confined by transverse reinforcement exhibits a more ductile behavior than its unconfined counterpart (Pauley and Priestley 1992, Park and Pauley 1975, Kent and Park 1971, Park *et al.* 1982). The first step, in order to generate moment-rotation characteristics for a section is therefore, to obtain the stress-strain curve for the confined concrete. Many researchers have proposed models to estimate the stress-strain curve for the confined concrete from mid twentieth century (Kent and Park 1971, Chan 1955, Baker and Amarakone 1964, Sargin *et al.* 1971) to late twentieth and early twenty first century (Park *et al.* 1982, Sheikh and Uzumeri 1982, Mander *et al.* 1988, Rueda and Elnashai 1997, Li *et al.* 2005). Many other models also may found in literature. However, out of all these models, the modified Kent and Park model (Park *et al.* 1982) and Mander model (Mander *et al.* 1988) are more popular, mainly because they offer a good balance between simplicity and accuracy. In this work, the modified Kent and Park model (Fig. 6) was followed, however the authors believe that the Mander model should also provide similar results. The stress-strain characteristics for the reinforcement steel used in this work considered strain hardening in the post yield portion of the curve (Fig. 7). Same curve was followed for reinforcement bars in tension and compression.

Once the stress-strain curves for steel and concrete are formulated, the moment-curvature characteristics of the section can be derived using the standard procedure, where the concrete strain at the extreme compression fiber, ε_{cm} is assumed and the force equilibrium between compressive

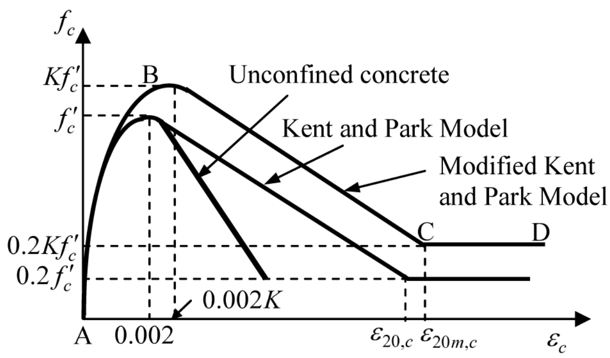

Fig. 6 Stress-strain curve for concrete

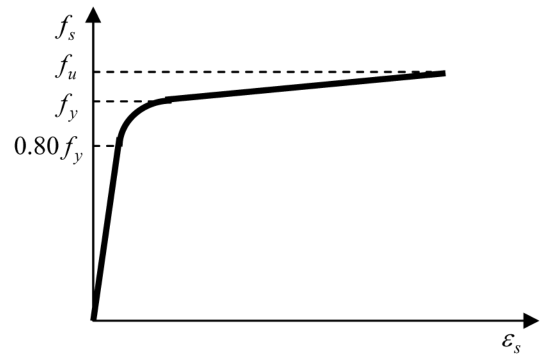

Fig. 7 Stress-strain curve for reinforcement

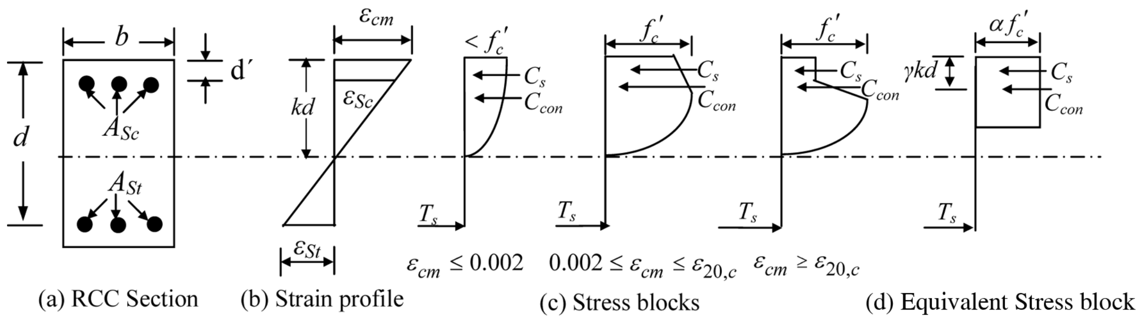

Fig. 8 Equivalent stress blocks corresponding to different extreme compression fiber strain

and tensile forces is established using iterative procedure to arrive at the correct neutral axis depth. The moment of resistance is then calculated by taking the moments of compressive and tensile forces about the centroid of the section and the corresponding curvature is obtained by dividing the extreme compression fiber strain by the neutral axis depth. In this work, the magnitude and point of application of compressive forces in concrete for various strain levels were calculated using the equivalent stress block approach (Fig. 8), since the sections were rectangular with constant width. The stress block parameter, α, and the neutral axis depth factor, γ, are calculated using following formulations.

$$\alpha = \frac{\int_0^{\varepsilon_{cm}} f_c d\varepsilon_c}{f_c' \varepsilon_{cm}} \tag{1}$$

$$\gamma = 1 - \frac{\int_0^{\varepsilon_{cm}} \varepsilon_c f_c d\varepsilon_c}{\varepsilon_{cm} \int_0^{\varepsilon_{cm}} f_c d\varepsilon_c} \tag{2}$$

The moment-curvature characteristics thus generated were converted to moment-rotation characteristics using the following formulations.

Yield rotation $$\theta_y = \int_0^L \varphi_y dx = \int_0^L \frac{M_y}{EI} dx \quad (3)$$

And ultimate rotation $$\theta_u = \theta_y + (\varphi_u - \varphi_y) l_p \quad (4)$$

where, l_p is the plastic hinge length, which was calculated using the formulation suggested by Baker for confined concrete (Park and Pauley 1975, Baker and Amarakone 1964). Alternatively, the expression suggested by Pauley and Priestley (1982) may also be used. However, for typical beam and column proportions, a value of l_p as, half of effective depth of the section, may be used with sufficient accuracy.

6.2 Shear force-deformation characteristics for members

To predict the shear force-deformation characteristics, an incremental analytical approach (Watanabe and Lee 1998) was followed. The model is based on the truss mechanism. In the analysis, the stirrup strain is gradually increased with a small increment and the resisting shear at each step is calculated. The stress state is characterized by a biaxial stress field in the concrete and a uniaxial tension field in the shear reinforcement. Kupfer and Bulicek (1992) theory for the equilibrium condition of stresses and compatibility condition of strains for the concrete element shown is followed. The equilibrium condition of stresses, compatibility condition of strains and constitutive laws are then used to obtain the complete shear force *v/s* deformation characteristics for the members. The method is straightforward and easily programmable. However, a detailed description of the approach is beyond the scope of this paper and the details of the model may be obtained from the reference (Watanabe and Lee 1998).

6.3 Joint characteristics

From equilibrium of the joint, as shown in Fig. 1(b), we get,
Horizontal joint shear force, V_{jh} is given by

$$V_{jh} = T_b - V_c \quad (1)$$

Where,
T_b is the tension force in the longitudinal beam reinforcement, and
V_c is the shear force on column
Now, we have

$$T_b = M_b/Z_b = V_b L_b/Z_b \quad (2)$$

Where,
M_b is the moment on the beam at column face,
Z_b is the lever arm
L_b is the length of the beam as shown in Fig. 1
V_b is the shear force on the beam
Also, from the equilibrium of external actions, we have

$$V_c = V_b(L_b + 0.5h_c)/L_c \quad (3)$$

Where,
h_c is the depth of the column and
L_c is the total length of column as shown in Fig. 1

Substituting (2) and (3) in (1), we get

$$V_{jh} = V_b\left(\frac{L_b}{Z_b} - \frac{L_b + 0.5h_c}{L_c}\right) \tag{4}$$

The horizontal joint shear stress, τ is given as

$$\tau = \frac{V_{jh}}{h_c' b_c'} \tag{5}$$

where, h_c' and b_c' are the length and width of joint core respectively.

In general, for sufficient accuracy, we can consider

$$Z_b = d_b - d_b' \tag{6}$$

Where,
d_b = Effective depth of the beam
d_b' = Effective cover to compression reinforcement

FEMA 356 (2000) gives the failure criteria in terms of horizontal joint shear stress (τ) *v/s* joint shear deformation. The shear stress values are given in terms of $k\sqrt{f_c'}$, where, f_c' is the cylinder compressive strength of concrete and k is a parameter that depends on the confinement provided by the members framing into the joint and joint reinforcement. The corresponding allowable horizontal joint shear force, V_{jh}, can be found from Eq. (5). Knowing the dimensions and details of the joint sub-assemblage, the corresponding force required in the beam end, V_b, can be calculated from Eq. (4) and $M_b = V_b L_b$ gives the corresponding moment at the beam end that corresponds to the failure of the joint. The beam end rotation due to joint deformation is same as the joint deformation itself.

This way, the joint shear deformation characteristics was converted to equivalent moment-rotation characteristics at beam end and that was provided as input to the program.

7. Comparison of experimental and analytical results

Figs. 9 and 10 present the results for joints 1 and 2 respectively. The weak-beam strong column joints are similar with the only difference being in the reinforcement detailing, joint 1 being unconfined and joint 2 being confined as per newer recommendations. The loading sequence for both the joints consisted of three cycles each of displacements of 3 mm, 6 mm, 9 mm and so on till failure. The test on joint 2 was restricted due to the limitation of the actuator stroke length and not because of degradation of joint. Both the joints attained a peak strength of similar order, which is as expected since the longitudinal reinforcement details are exactly same for the two joints and the joints underwent a typical flexural failure. The major difference is observed in the post peak behavior of the two joints. The hysteretic loops and envelope for joint 1 shows significant strength degradation immediately after attaining peak, whereas for joint 2, the strength degradation is much less even after peak. The analytical plots for joints 1 and 2 also show a similar response, since the

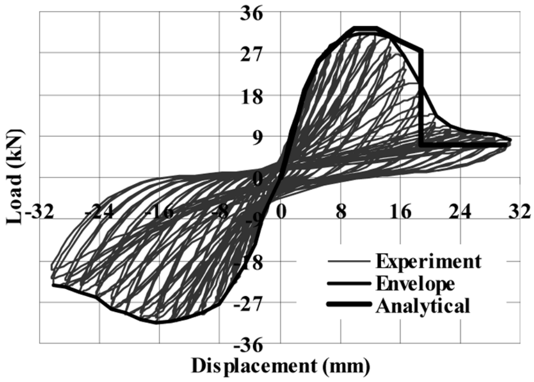

Fig. 9 Results for Joint 1

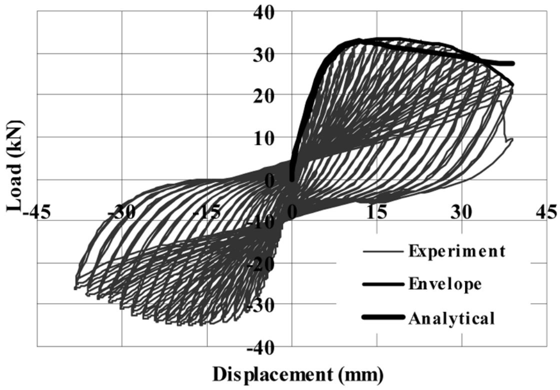

Fig. 10 Results for Joint 2

modified Kent and Park model gives due consideration to the effect of transverse reinforcement spacing on ductile behavior of concrete. The ultimate displacement is assigned as the displacement corresponding to a 20% drop of lateral load capacity from the maximum value as recommended by Priestly and Park (1987).

The failure mode of the joints may be predicted analytically by comparing the load required to produce hinges in beam and columns under different modes. From the moment-rotation and shear force-deformation analysis for beam sections, we get the yield moment and shear force for Joint 1 as 15.40 kNm and 28.83 kN and for Joint 2 as 15.40 kNm and 33.63 kN respectively. Yield loads for flexural failure mode for the joints can be calculated by dividing yield moment by beam length. For both joints, yield load for flexural failure is thus equal to 25.67 kN. Similarly for shear failure mode, the yield load may be obtained by subtracting the self-weight of the beam (approx 0.5 kN) from yield shear force. Thus for joint 1, the yield load from shear failure point of view is 28.33 kN and that for joint 2 is 33.13 kN. A similar calculation for columns show that the columns are much stronger in both flexure and shear as compared to the beam. Thus, we can predict that the yielding of both the joints should commence in a flexure failure mode at a load of around 25.67 kN, which is same as experimentally obtained yield load (see Figs. 6 and 7). However, since for joint 1, the yield load for shear failure is also close by (28.33 kN), good amount of flexure-shear cracks are expected, which actually happened in the experiment. For joint 2, since the yield shear load is quite far away and is almost equal to the ultimate load in flexure mode too, for this joint mainly flexure mode is expected to govern, again supported by evidence from tests. Thus, a simple and basic calculation can give an idea, if not complete detail, about the failure modes of the joints, without actually following fracture mechanics approach.

Figs. 11 and 12 show the failure photographs for the two joints. It can be seen that, in Joint 1, there is a significant amount of concrete spalling from the beam and the beam-column junction, mainly due to flexure-shear cracks, which is basically responsible for strength degradation observed in hysteretic plots for the joint. The cracking and spalling started first in the beam (as expected by failure mode prediction) adjacent to the face of the column and then propagated to the junction. For joint 2, as can be seen from Fig. 12, there is very less amount of spalling and the crack propagation in the junction is also very less significant (characteristics of a typical flexural failure mode). This explains the insignificant post peak strength reduction of the joint. The experiment on this set of

Fig. 11 Damaged state of Joint 1

Fig. 12 Damaged state of Joint 2

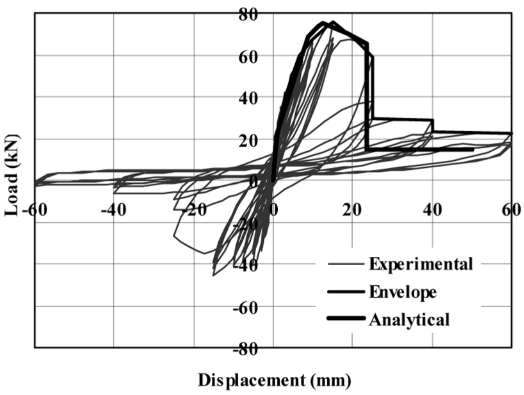

Fig. 13 Results for Joint 3

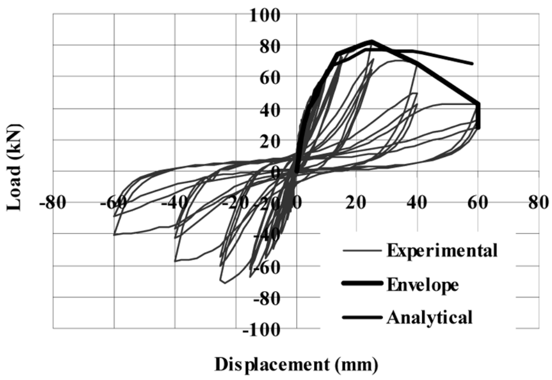

Fig. 14 Results for Joint 4

joint clearly brings out the benefits of following ductile detailing philosophy for the RC structures during cyclic loads such as caused due to earthquakes. Moreover, the analysis procedure described is able to predict the response of both confined and unconfined joints nicely.

Figs. 13 and 14 present the results for joints 3 and 4 respectively. The weak-column strong-beam joints are similar with the only difference being in the reinforcement detailing, joint 3 being unconfined and joint 4 being confined as per newer recommendations. The load sequence consists of three cycles each of 1 mm, 2 mm, 3 mm, 5 mm, 7.5 mm, 10 mm, 15 mm, 25 mm, 40 mm and 60 mm displacement amplitudes. Again a major difference is observed in the post peak behavior of the two joints. The hysteretic loops and envelope for joint 3 shows significant strength degradation immediately after attaining peak, whereas for joint 4, the strength degradation is much less. The hysteretic loops for joint 4 are much well formed with less pinching as compared to joint 3. The analytical plots for joints 3 and 4 also show a similar response.

Following similar calculations as done for joints 1 and 2, for failure mode prediction, we get that Joint 3 is dominated by flexural-shear failure of the column, while joint 4 is dominated by flexural failure of column only, with good margin against shear failure. Similar observations were made from tests too. In joint 3, the damage was mainly concentrated in the beam-column joint region and the beam stub had suffered much lesser damage mainly due to the fact that the joint had a strong-beam weak-column configuration. At about 25 mm displacement excursion, there was a sudden drop in the strength of the specimen, though the specimen sustained cyclic loading up to three

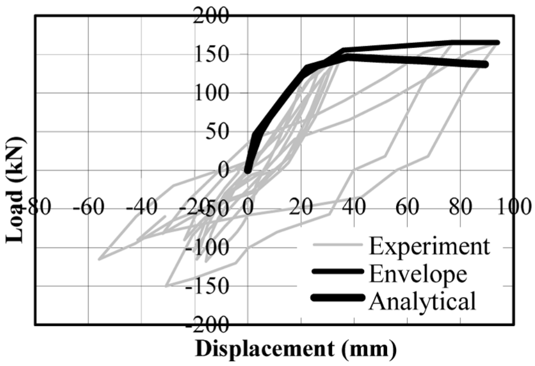

Fig. 15 Results for Joint 5

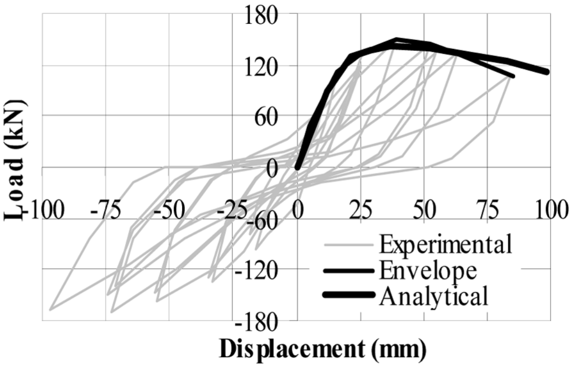

Fig. 16 Results for Joint 6

cycles of 60 mm displacement excursions without any failure in reinforcing bars. After three cycles, the test was stopped as the strength of the specimen dropped to around less than a third of its ultimate strength. In joint 4, at lower displacement excursions there was significant cracking in the beam, column and joint region. The flexural cracks in the beams were spread uniformly till the end of beam stub, but at higher displacement excursions the damage was primarily found in the joint region. However, the strength degradation was much less in this joint even at high displacement excursions. The test was stopped due to the limitation of stroke length of actuator. As far as analytical evaluation of the response for the joints is concerned, it is again found that the analytical results follow the experimental results closely till failure. The main attraction in the analytical results is the agreement between analytical and experimental plots in the post peak region. Again the codal recommendations for increased ductility were found to be valid.

The experimental and analytical results for joints 5 and 6 are shown in Figs. 15 and 16 respectively. Both the joints have similar sizes and details except for the lateral ties spacing in column, which are closely spaced in joint 6 as compared to joint 5.

The sizes of both beam and column were 400 mm by 400 mm, which is more realistic as compared to previous four joints. Joint 5 shows a pinched behavior and the hysteretic loops are quite unsymmetric about both the axes. This is because of the fact that the compression bars (bottom bars) were not anchored at the face of the column and the detailing was meant for resisting gravity loads only as per the recommendations of old codes. However, the hysteretic loops for joint 6 are only marginally unsymmetric in the two directions, since both the top and bottom bars are properly anchored as per the recommendations of newer codes. The experimental and analytical values of initial slopes, yield load and displacement and ultimate loads were found to be in good agreement. However, the ultimate displacement value for joint 6 was found to be somewhat on higher side due to the inherent assumption in the stress-strain model for concrete that closer stirrup spacing leads to higher ultimate displacement.

By calculating loads corresponding to various failure modes, failure pattern is found to be mainly flexural failure and flexural-shear failure of column for both the joints with a little more margin against shear for joint 6. Similar behavior was found experimentally.

The crack patterns for the two joints are shown in Figs. 17 and 18 respectively. It can be seen that numerous cracks have developed in the column and the beam-column joint region, however, there is relatively less cracking in the beam stub. This is again as expected due to weak-column strong-

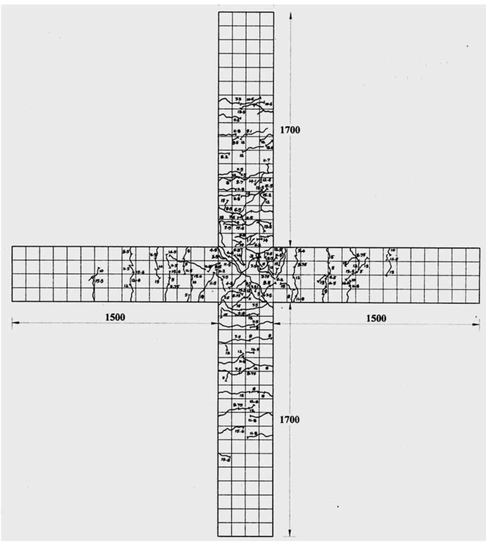

Fig. 17 Crack Pattern for Joint 5

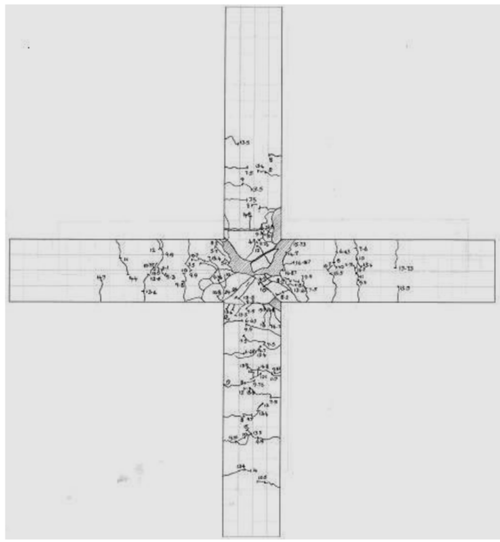

Fig. 18 Crack Pattern for Joint 6

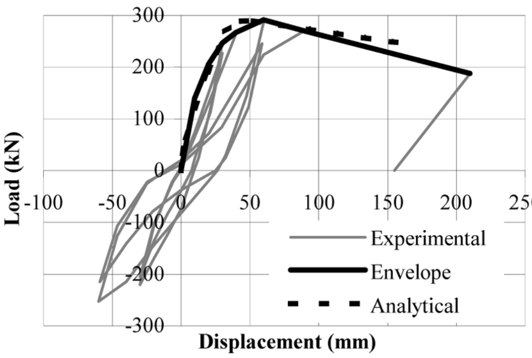

Fig. 19 Results for Joint 7

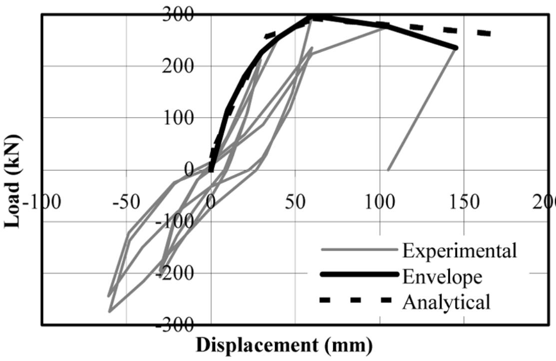

Fig. 20 Results for Joint 8

beam design. The number of cracks developed were more in joint 5, however in joint 6, spalling of concrete took place from beam-column joint region which was responsible for post peak strength degradation.

Joints 7 and 8 were both exterior (Tee-shaped) joints with beam dimensions slightly greater than those in joints 5 and 6 (Table 1). Both the joints were of strong-beam weak-column configuration, with joint 7 designed and detailed as per old codes and joint 8 detailed as per newer codes with closer stirrups and lateral ties. The loading given to these joints was corresponding to high displacement cycles with first two cycles of 30 mm and next two cycles of 60 mm. After that the displacement were increased gradually till failure. The hysteretic characteristics of both the joints were found to be very similar (Figs. 19 and 20). Both the joints exhibited severe pinching in 2nd cycle of 60 mm displacement. The ultimate load, yield load and yield displacements and the post peak behavior are similar for both the cases. The displacement corresponding to 20% strength degradation is also very close for both.

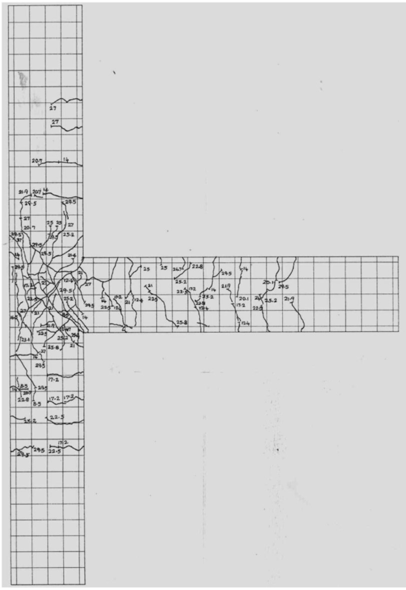
Fig. 21 Crack Pattern for Joint 7

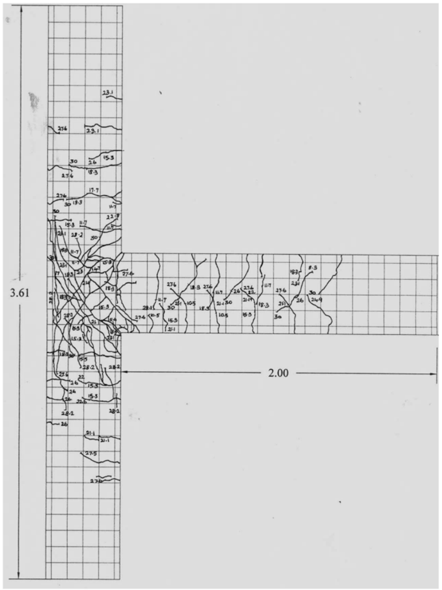

Fig. 22 Crack Pattern for Joint 8

The failure pattern predicted by calculating loads corresponding to various failure modes is found to be flexural failure of column followed by flexural-shear failure of beam for both the joints with a little more margin against shear for joint 8. Similar behavior was found experimentally.

Figs. 21 and 22 show the crack pattern for the two joints. Severe shear cracks were observed in the joint region for both the joints. Thus under high stress cycles, the two joints displayed a very similar behavior and any significant effect of different types of detailing is not observed. As far as the analytical behavior is concerned, a little difference in the post peak behavior is observed but it is not very significant. However, again for both the cases, the analytical results match closely with the experimental ones.

9. Observations

From the experiments and analysis of the joints, the following observations could be made:

1. The confined detailing improves the behavior of small-scale joints significantly.
2. Confined detailing for small joints improves post peak behavior by checking strength degradation, and also helps in formation of well-formed hysteretic loops with less pinching.
3. Any significant change in the strength of the joints due to confined detailing is not observed unlike axial strength increase of columns due to confinement by closely spaced ties.
4. The effect of confined detailing is much less pronounced on larger (real life scale) joints and higher ductility for joints having confined detailing is not warranted. This may be attributed to the fact that for larger sized joints, the dominance of shear failure mode increases.
5. Pre and post peak behavior of larger joints is similar for both confined and unconfined joints.
6. The hysteretic behavior of both small and large unconfined joints even with equal top and bottom reinforcement is generally quite unsymmetrical about both the axes due to lack of

anchorage for compression reinforcement.

7. More number of cracks in joints were observed in weak-column strong-beam configuration.
8. The analytical procedure described in the paper is capable of providing vital information on strength and ductility of the joints (and can be easily extended to structures).
9. Although there may be a slight mismatch in the ultimate displacement for larger joints, the displacement corresponding to 20% strength degradation is found to be in excellent agreement with experimental results.
10. The simple calculations for failure loads of individual components can be used to get useful information about the failure pattern of joints.

10. Conclusions

The experimental work carried out and presented in this paper throws light on an important aspect from the point of view of structural safety of structures under cyclic loads. To begin with, this experimental programme further verified the fact already proven by earlier researchers that the confined detailing does improve the ductility of reinforced concrete members and joints. But this conclusion is limited to small laboratory sized joints only. For such joints, the confined detailing improves the post-peak behavior by inducing larger ductility and forming well-defined hysteretic loops, but it does not affect the peak strength of the joint significantly. However, the effectiveness of confined detailing on behavior of joints reduces significantly as we go for larger real life sized members, for which similar kinds of ductility values, as found for unconfined joints, were noted. This may be due to shear dominance in larger sized joints. However, more such tests are recommended to arrive at a sound conclusion in this regard. The analytical method presented in this paper based on the classical approach using nonlinear static pushover analysis is an easy-to-use and effective tool to gather the information on complete nonlinear behavior of RC structures. Moreover the method gives important information about the failure modes for the joint too.

Acknowledgements

The authors highly acknowledge the efforts of Prof. Abhijit Mukherjee, Thapar Institute of Technology (Ex Prof IIT Bombay), Prof. S.K. Jain and Prof. C.V.R. Murthy, IIT Kanpur, Dr. Thandavamoorthy, SERC Chennai and their teams for conducting the required tests. We thank BRNS to support the research work by granting required funds. In the end, the very valuable comments obtained from the reviewer's are highly acknowledged that helped in improving the quality of the content of the paper.

References

Pauley, T. and Priestley, M.J.N. (1992), *Seismic Design of Reinforced Concrete and Masonry Buildings*, John Wiley and Sons, New York.

ACI 318M-08 (2008), "Building code requirements for reinforced concrete", American Concrete Institute, Detroit, Michigan.

FEMA 356 (2000), *NEHRP Guidelines for the Seismic Rehabilitation of Buildings*, Federal Emergency Management Agency, Washington DC.

Eurocode 8 (2003), *Design of Structures for Earthquake Resistance - Part 1: General Rules, Seismic Actions and Rules for Buildings*, European Standard Final Draft PrEN 1998-1.

NZS 3101:1995 (1995), *New Zealand Standard Concrete Structures Standard part 1-The Design of Concrete Structures*, Standards Association of New Zealand.

IS 13920:1993 (2002), "Indian Standard Ductile Detailing of Reinforced Concrete Structures Subjected to Seismic Forces - Code of Practice", Edition 1.2, Bureau of Indian Standards.

IS 456:2000 (2000), "Indian Standard Plain and Reinforced Concrete - Code of Practice (Fourth Revision)", Bureau of Indian Standards.

Hanson, N.W. and Connor, H.W. (1967), "Seismic resistance of reinforced concrete beam-column joints", *J. Struct. Div-ASCE*, **93**(5), 533-560.

Renton, G.W. (1972), *The behavior of Reinforced Concrete Beam-column Joints under Cyclic Loading*, Master of Engineering Thesis, University of Canterbury, Christchurch, New Zealand.

Park, R. and Pauley, T. (1975), *Reinforced Concrete Structures*, John Wiley and Sons.

Park, R. and Thompson, K.J. (1974), *Behavior of Prestressed, Partially Prestressed and Reinforced Concrete Interior Beam-column Assemblies under Cyclic Loading: Test Results of Units 1 to 7*, Research Report 74-9, Department of civil Engineering, University of Canterbury.

Lee, D.L.N., Wight, J.K. and Hanson, R.D. (1977), "RC beam-column joints under large load reversals", *J. Struct. Div-ASCE*, **103**(12), 2337-2350.

Leon, R.T. (1990), "Shear strength and hysteretic behavior of interior beam-column joints", *ACI Struct. J.*, **87**(1), 3-11.

Raffaelle, G.S. and Wight, J.K. (1995), "Reinforced concrete eccentric beam-column connections subjected to earthquake type loading", *ACI Struct. J.*, **92**(1), 45-55.

Satish Kumar, S.R. and Vijaya Raju, B. (2002), "Hysteretic behavior of lightly reinforced concrete exterior beam-to-column joint sub-assemblages", *J. Struct. Eng., Struct. Eng. Res. Centre*, **29**(1), 31-37.

Megget, L.M. (2003), "The seismic design and performance of reinforced concrete beam-column knee joints in buildings", *Earthq. Spectra*, **19**(4), 863-895.

Mukherjee, A. (2006), *Upgradation of Concrete Structures with Fiber Reinforced Composites*, Report for Project No. 05, Board of Research in Nuclear Sciences, Indian Institute of Technology Bombay.

Jain, S.K. and Murty, C.V.R. (1999), *Experimental Investigation of Cyclic Behavior of RC Flexural Members*, Consolidated Technical Report for Atomic Energy Regulatory Board, Indian Institute of Technology Kanpur.

Thandavamoorthy *et al.* (2006), *Investigations on the Inelastic Behavior of RC Beam-Column Joint under Cyclic Reversals*, Completion Report for Board of Research in Nuclear Sciences, Project No. GAP 01141, Structural Engineering Research Centre, Chennai.

Kent, D.C. and Park, R. (1971), "Flexural members with confined concrete", *J. Struct. Div-ASCE*, **97**(7), 1969-1990.

Park, R., Priestley, M.J.N. and Gill, W.D. (1982), "Ductility of square-confined concrete columns", *J. Struct. Eng-ASCE*, **108**(4), 929-950.

Chan W.L. (1955), "The ultimate strength and deformation of plastic hinges in reinforced concrete frameworks", *Mag. Concrete Res.*, **7**(21), 121-132.

Baker, A.L.L. and Amarakone, A.M.N. (1964), "Inelastic Hyperstatic Frames Analysis", *Proceedings of the International Symposium on the Flexural Mechanics of Reinforced Concrete*, Miami, November.

Sargin, M., Ghosh, S.K. and Handa, V.K. (1971), "Effects of lateral reinforcement upon the strength and deformation properties of concrete", *Mag. Concrete Res.*, **23**(75-76), 99-110.

Sheikh, S.A. and Uzumeri, S.M. (1982), "Analytical model for concrete confinement in tied columns", *J. Struct. Div-ASCE*, **108**(12), 2703-2722.

Mander, J.B., Priestley, M.J.N. and Park, R. (1988), "Theoretical stress-strain behavior of confined concrete", *J. Struct. Eng-ASCE*, **114**(8), 1804-1826.

Rueda, J.E.M. and Elnashai, A.S. (1997), "Confined concrete model under cyclic load", *Mater. Struct.*, **30**(3), 139-147.

Li, Y.F., Chen, S.H., Chang, K.C. and Liu, K.Y. (2005), "A constitutive model of concrete confined by steel reinforcements and steel jackets", *Can. J. Civil Eng.*, **32**, 279-288.

Watanabe, F. and Lee, J.Y. (1998), "Theoretical prediction of shear strength and failure mode of reinforced concrete beams", *ACI Struct. J.*, **95**(6), 749-757.

Kupfer, H. and Bulicek, H. (1992), "A consistent model for the design of shear reinforcement in slender beams with I- or Box-shaped cross section", *Proceedings of the International Workshop on Concrete Shear in Earthquake*, Houston.

Priestley, M.J.N. and Park, R. (1987), "Strength and ductility of concrete bridge columns under seismic loading", *ACI Struct. J.*, **84**(1), 61-76.

Priestley, M.J.N. (1997), "Displacement based seismic assessment of reinforced concrete buildings", *J. Earthq. Eng.*, **1**(1), 157-192.